Control of bulk superconductivity in a BCS superconductor by surface charge doping via electrochemical gating

E. Piatti,[1] D. Daghero,[1] G. A. Ummarino,[1,2] F. Laviano,[1] J. R. Nair,[1] R. Cristiano,[3] A. Casaburi,[4] C. Portesi,[5] A. Sola,[5] and R. S. Gonnelli[1,*]

[1]*Department of Applied Science and Technology, Politecnico di Torino, Torino, Italy*
[2]*National Research Nuclear University MEPhI, Moscow Engineering Physics Institute, Moscow, Russia*
[3]*CNR-SPIN Institute of Superconductors, Innovative Materials and Devices, UOS-Napoli, Napoli, Italy*
[4]*School of Engineering, University of Glasgow, Glasgow, United Kingdom*
[5]*INRIM—Istituto Nazionale di Ricerca Metrologica, Torino, Italy*

The electrochemical gating technique is a powerful tool to tune the surface conduction properties of various materials by means of pure charge doping, but its efficiency is thought to be hampered in materials with a good electronic screening. We show that, if applied to a metallic superconductor (NbN thin films), this approach allows the observation of reversible enhancements or suppressions of the bulk superconducting transition temperature, which vary with the thickness of the films. These results are interpreted in terms of a proximity effect, and indicate that the effective screening length depends on the induced charge density, becoming much larger than that predicted by a standard screening theory at very high electric fields.

The field effect (i.e., the modulation of the conduction properties of a material by means of a transverse electric field) is widely used in semiconducting electronic devices, namely, field-effect transistors (FETs). Recently, unprecedented intensities of the electric field—and thus densities of induced charge—have been reached by exploiting the formation of an electric double layer (EDL) at the interface between an electrolyte and the solid, when a voltage is applied between the latter and a gate electrode immersed in the electrolyte. The EDL acts as a nanoscale capacitor with a nanometric spacing between the "plates", so that the electric field can be orders of magnitude higher than in standard field-effect (FE) devices. In these extreme conditions, new phases (including superconductivity) have been discovered in various materials, mostly semiconducting or insulating in their native state [1–5]. Instead, high-carrier-density systems such as metals and standard BCS superconductors have so far received little attention, because the electronic screening strongly limits the FE. A few works on gold [6,7] and other noble metals [8] remain the only literature about EDL gating on normal metals. More exotic metallic systems, i.e., two-dimensional (2D) materials of different classes [9–13] and complex oxides [14–20], were explored more extensively. In particular, the microscopic mechanism behind the carrier density modulation in EDL-gated oxides remains a subject of investigation [19,21–23].

The FE on BCS superconductors was investigated in the 1960's via solid dielectric [24] and ferroelectric [25] gating, and small (positive or negative) variations of the superconducting transition temperature (T_c) were observed on increasing/decreasing the charge carrier density. Recent EDL gating experiments in Nb thin films [26] gave evidence of completely reversible T_c shifts about three orders of magnitude larger than in Refs. [24,25], though still smaller than 0.1 K. Despite the very effective electronic screening (due to unpaired electrons) the suppression of T_c was visible also in films

as thick as 120 nm. This means that the superconducting properties of the bulk were somehow changed by the applied gate voltage; otherwise, the surface layer with reduced T_c would have been shunted by the underlying bulk, giving no visible effect on the transition. A proper understanding of how this could happen is, however, still lacking [26].

In this Rapid Communication we suggest a solution to this problem—that first appeared in the literature more than 50 years ago [24,25]—by studying the T_c modulation of NbN thin films under EDL gating for different values of the film thickness t. We find that the T_c shift depends on t, thus proving that the whole bulk comes into play. If the proximity effect is taken into account within the strong-coupling limit of the standard BCS theory, this finding turns out to be compatible with a charge induction limited to the surface. We also find evidence suggesting that the volume density of the induced charge Δn_{3D} does not increase indefinitely with the gate voltage, but saturates at a maximum of about 0.4 electrons per unit cell—while no saturation occurs in the surface charge density Δn_{2D}. Thus, the electrostatic screening length increases with the gate voltage, becoming much larger than the Thomas-Fermi screening length λ_{TF} when $\Delta n_{2D} > 2 \times 10^{15}$ cm^{-2}.

NbN thin films were grown on insulating MgO substrates by reactive magnetron sputtering. The device geometry was defined by photolithography and subsequent wet etching in a 1:1 HF:HNO$_3$ solution. The inset to Fig. 1(a) shows the scheme of the samples: The strip is 135 μm wide, with current pads on each end and four voltage contacts on each side, spaced by 946 μm from one another. This geometry allows one to measure the voltage drop across different portions of the strip at the same time, thus defining an active (gated) and a reference (ungated) channel.

The film thickness t was measured by atomic force microscopy (AFM). Figure 1(a) shows the sheet resistance $R_\square$ of the pristine film ($t = 39.2 \pm 0.8$ nm) versus temperature. The nonmonotonic behavior of $R_\square(T)$ and the residual resistivity ratio RRR = $R(300$ K$)/R(16$ K$) = 1.05$ are characteristic of
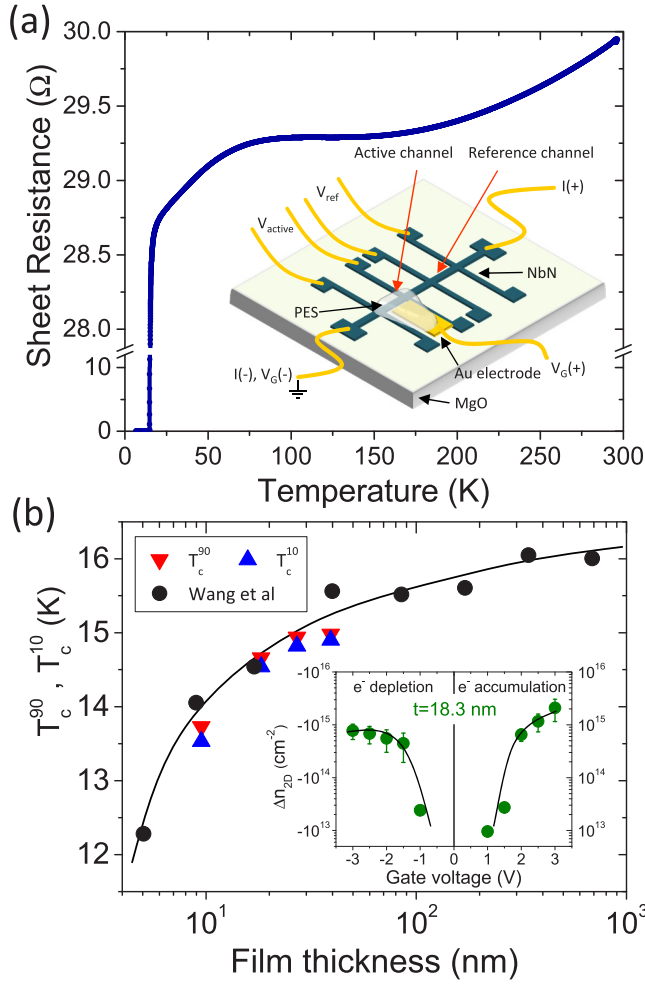
FIG. 1. (a) Sheet resistance $R_\square$ as a function of temperature for the pristine 39.2-nm-thick device (prior to the PES deposition). The inset shows a scheme of the complete device. (b) T_c as a function of the film thickness: Both T_c^{90} (down triangles) and T_c^{10} (up triangles) are reported to show the variation in the transition width. Black dots are data taken from the literature [29]. Inset: Typical Δn_{2D} vs V_G curve determined by chronocoulometry.

granular NbN films of fairly high quality [27]. Subsequent steps of Ar-ion milling were used to reduce the thickness to 27.1 ± 1.5, 18.3 ± 1.7, and finally 9.5 ± 1.8 nm [28]. On reducing t, T_c was suppressed [in good agreement with the curve for NbN films reported in the literature [29]; see Fig. 1(b)] and the transition width slightly increased. Both these effects are consistent with the fact that t approaches the coherence length of the material [29].

To perform EDL gating measurements, we covered the active channel and the gate counterelectrode placed on its side [made of a thin Au flake; see the inset to Fig. 1(a)] with the liquid precursor of the cross-linked polymer electrolyte system (PES), which was later UV cured.

Nb-based compounds always present a thin oxide layer at the surface (see Ref. [30] and references therein); in NbN this layer is less than 1 nm thick [30], and does not significantly reduce the gate capacitance. Indeed, EDL gating experiments performed through a thin insulating layer [13,31] indicate that

it actually minimizes the (unwanted) electrochemical reactions between sample and electrolyte.

To determine the surface electron density Δn_{2D} induced by a gate voltage V_G, we used the well-established electrochemical technique called double-step chronocoulometry [32]. We applied a given V_G at room temperature (above the glass transition of the PES, which occurs below 230 K) as a step perturbation, and then removed it. As shown in Ref. [33], an analysis of the gate current as a function of time allowed us to separate the contribution due to diffusion of electroreactants from that due to the EDL buildup; from the latter, one can determine the charge stored in the EDL and thus Δn_{2D}. A typical Δn_{2D} vs V_G curve is shown in the inset to Fig. 1(b). The reproducibility of the Δn_{2D} estimation for multiple subsequent applications of the same V_G is within $\sim 30\%$ of the value, comparable with the uncertainty on Δn_{2D} of the technique itself [6].

To measure the effect of a given V_G on the transition temperature, we applied V_G at room temperature and kept it constant while cooling the device down to 2.7 K in a pulse-tube cryocooler. The voltage drops across the active and the reference channel, V_{active} and V_{ref} [see the inset to Fig. 1(a)], were then measured simultaneously during the very slow, quasistatic heating up to room temperature in the presence of a source-drain dc current of a few μA. By comparing the $R_\square(T)$ curves of the active and reference channels measured at the same time, we were able to eliminate the possible small differences in critical temperature measured in different heating runs, and thus to detect shifts in T_c due to EDL gating as small as a few mK. For instance, the T_c shift due to $V_G = +3$ V was evaluated as $\Delta T_c(3\text{ V}) = [T_c^{\text{active}} - T_c^{\text{ref}}]_{V_G=3\text{ V}} - [T_c^{\text{active}} - T_c^{\text{ref}}]_{V_G=0\text{ V}}$.

Figure 2(a) shows, as an example, the effect of a gate voltage ranging between $+3$ and -3 V on the superconducting transition of the 18.3-nm-thick film. The horizontal scale is the temperature normalized to the midpoint of the transition in the reference channel, i.e., $[T - T_c^{\text{ref}}]_{V_G} - [T_c^{\text{active}} - T_c^{\text{ref}}]_0$. As for all thicknesses, the gate voltage reproducibly produces a rigid shift of the transition to a lower (higher) temperature for positive (negative) V_G, respectively. The amplitude of the reversible shift [28] is clearly correlated with the induced charge density.

Figure 2(b) shows that the amplitude of the T_c shift produced by a given gate voltage (here, $+3.0$ and -3.0 V) is enhanced when the thickness t is reduced. This (together with the detection of negative T_c shifts for positive V_G) suggests that the superconducting properties of the whole bulk are affected by the surface charge induction. The values of ΔT_c vs Δn_{2D} for the different thicknesses are shown in Fig. 3.

Interestingly, the transition width depends on t but not on the gate voltage, indicating that the superconducting properties of the film are homogeneously modulated by the charge induction. The question then is how the electric field can induce this homogeneous perturbation in the whole thickness even in the presence of a strong electronic screening.

It is generally accepted that, at least in the limit of "weak" perturbations and linear response, the screening length in the superconducting state is the same as in the normal state, i.e., the Thomas-Fermi length [34]. This is certainly true in proximity
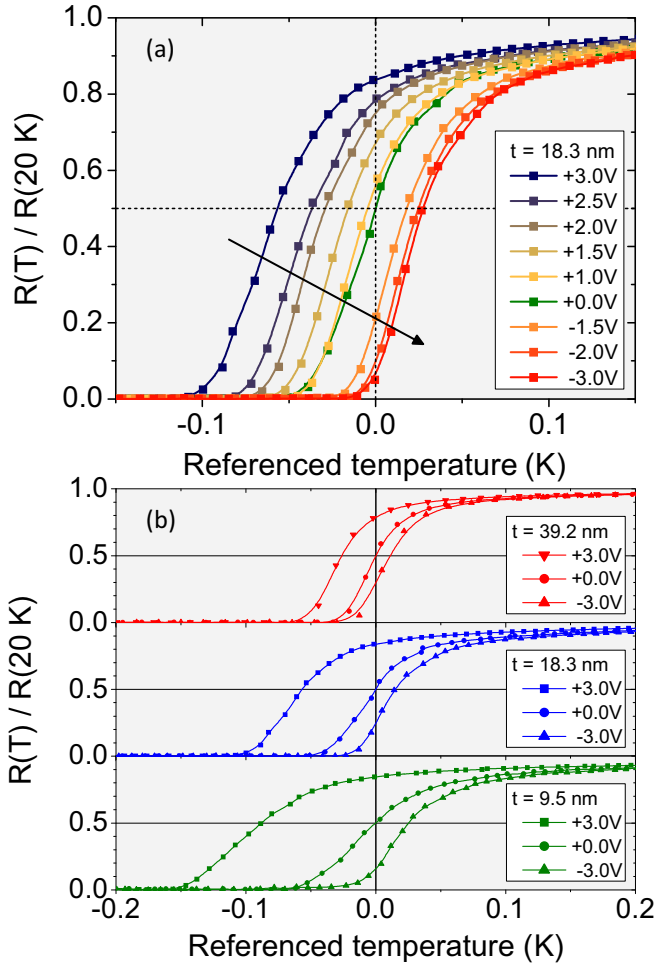
FIG. 2. (a) Normalized resistance $R(T)/R(20 \text{ K})$ of the active channel of a 18.3-nm-thick device, as a function of referenced temperature T^*, i.e., $T^* = [T - T_c^{\text{ref}}]_{V_G} - [T_c^{\text{active}} - T_c^{\text{ref}}]_0$, at different gate voltages in the range $[-3 \text{ V}, +3 \text{ V}]$. (b) Effect of a gate voltage $V_G = \pm 3$ V on the $R(T)/R(20 \text{ K})$ vs T curve for three values of thickness: 39.2, 18.3, and 9.5 nm.

FIG. 3. T_c shift, ΔT_c, as a function of the induced surface electron density Δn_{2D}, for all the film thicknesses. Dashed lines are only guides to the eye.

of T_c (i.e., at most 100 mK below it), where the screening is dominated by unpaired electrons since the superfluid density is very small [35]. We can thus safely assume that the electric field should decay at the NbN surface within a depth of the order of $\lambda_{\text{TF}} \simeq 1$ Å.

The most likely mechanism able to turn the perturbation of the carrier density in a thin surface layer into a homogeneous perturbation of the bulk superconducting properties is the proximity effect at a normal metal/superconductor interface. In general, this is observed as the induction of a superconducting order parameter in the normal bank (close to the interface) accompanied by its suppression in the superconducting one [36]. Moreover, when the thicknesses of the two banks are sufficiently small (Cooper limit [37]), the compound slab behaves as a homogeneous superconductor whose effective electron-phonon coupling constant $\langle \lambda \rangle$ is a weighted average of the coupling constants in the superconductor and in the normal metal [36,37]. From a scaling analysis of ΔT_c on the thicknesses of the two banks (as explained below), we determine that the models for the proximity effect in the
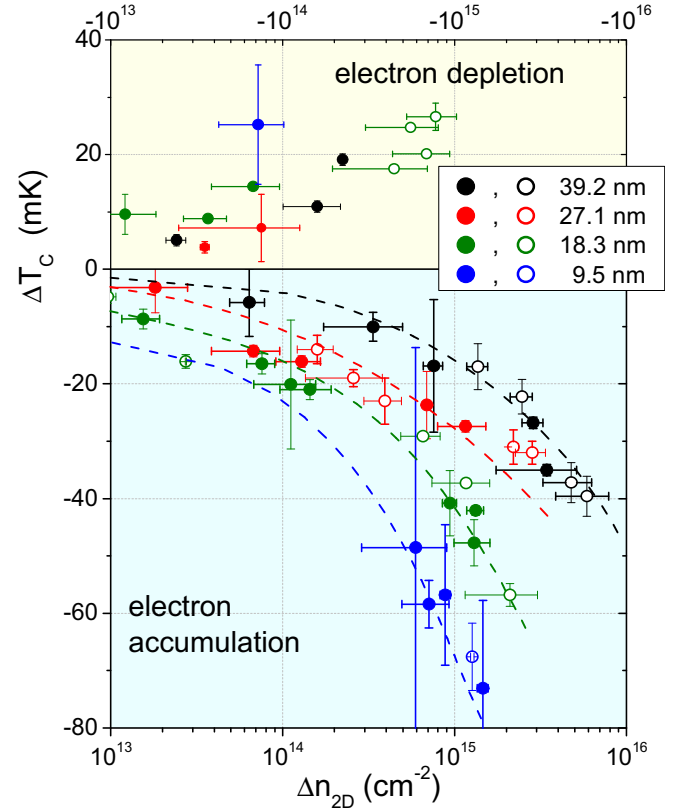
Cooper limit can be applied to our films [38]. Since NbN is a strong-coupling superconductor, we will actually use the strong-coupling version of the relevant model.

As a first approximation we can assume that both the characteristic temperature Θ (representative of the phonon spectrum and thus related to the Debye temperature) and the Coulomb pseudopotential μ^* are unaffected by the applied electric field, so that they can be obtained from literature [39]. Hence the model of Ref. [38] gives for the critical temperature of the compound slab,

$$T_{c,\text{comp}} = \frac{\Theta}{1.45} \exp\left[-\frac{1 + \langle \lambda \rangle}{\langle \lambda \rangle - \mu^*} \right], \quad (1)$$

where

$$\langle \lambda \rangle = \frac{\lambda_s N_s d_s + \lambda_b N_b d_b}{N_s d_s + N_b d_b} = \beta_s \lambda_s + \beta_b \lambda_b. \quad (2)$$

Here, the subscripts s and b refer to surface and bulk, $N_{s,b}$ are the densities of states (DOS) at the Fermi level, $\lambda_{s,b}$ the electron-phonon coupling constants, and $d_{s,b}$ the thicknesses of the layers, such that $d_s + d_b = t$. The condition under which the Cooper-limit model can be used [38] is that ΔT_c scales on the ratio d_b/d_s, which is true in our case (see Fig. S5) [28]. We assume the effect of the induced charge on T_c to be mainly due to the modulation of N_s/N_b: Therefore, the coupling strength can be expressed in the simplest way as $\lambda_s = \lambda_b(N_s/N_b)$, λ_b being calculated from the unperturbed T_c through the McMillan equation. The only remaining unknown
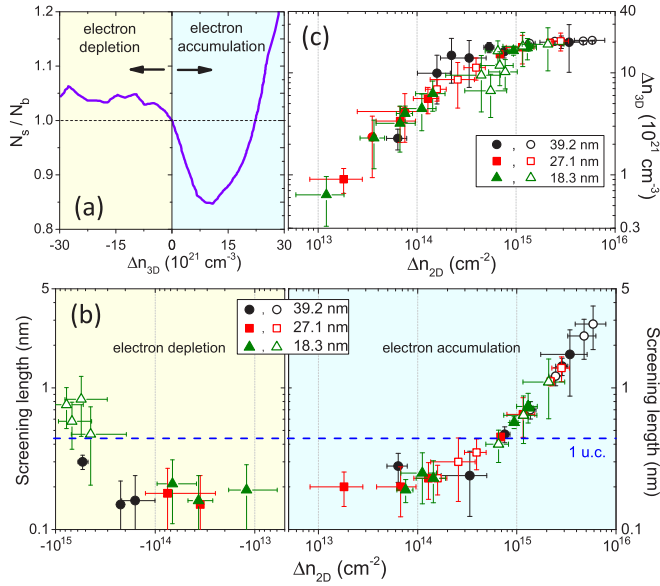
FIG. 4. (a) DOS ratio N_s/N_b of NbN as a function of Δn_{3D} (i.e., $\Delta n_{3D} = 0$ corresponds to native NbN). (b) Thickness of the perturbed surface layer d_s vs Δn_{2D} for both electron accumulation and depletion. The horizontal dashed line indicates the size of one unit cell of NbN. (c) Absolute value of the volume density of induced electrons (in the surface layer) Δn_{3D} as a function of Δn_{2D}.

quantity is thus the DOS ratio N_s/N_b, which can be calculated via density functional theory (DFT) once the shift of the Fermi level from the ungated value is known [see Fig. 4(a)]. This shift is determined by the volume density of induced carriers Δn_{3D}, while double-step chronocoulometry is able to measure the surface charge density $\Delta n_{2D} = \int_0^t \Delta n_{3D}(z)dz$ [6]. An ansatz about how the volume charge density distributes across the thickness is thus required to determine N_s/N_b.

Since within the model in Ref. [38] the two layers of the compound slab are homogeneous, we choose for $\Delta n_{3D}(z)$ a step profile, i.e., we assume the induced charge to be uniformly distributed in a thickness d_s, which is an adjustable parameter of our model. d_s can thus be considered an effective electrostatic screening length. For any value of Δn_{2D}, the choice of d_s determines Δn_{3D} and, consequently, (i) (by DFT calculations) the shift of the Fermi level and the perturbed DOS ratio at the surface N_s/N_b, (ii) the electron-phonon coupling strength λ_s, (iii) the value of $T_{c,s}$, and finally the critical temperature of the compound slab $T_{c,comp}$ which has to agree with the experimental T_c.

The values of d_s that allow fitting the experimental T_c shifts are plotted as a function of Δn_{2D} in Fig. 4(b). Symbols of different shapes refer to different film thicknesses t. We excluded from our analysis the data for $t = 9.5$ nm as we

deem the measured T_c shift not to be reliable enough due to a pronounced hysteresis of the field effect [28]. It is clearly seen that d_s does not depend on t, which is reasonable, but must vary with Δn_{2D}. Let us focus on the electron accumulation side, where the trend is clearer. In the low-carrier-density region, d_s roughly agrees with the Thomas-Fermi screening length λ_{TF} if the density of quasiparticles at $T \simeq T_c$ is used, but already at 7×10^{14} cm^{-2} it becomes as large as one unit cell (4.4 Å). Without this increase in d_s, the volume charge density Δn_{3D} would become so large that the Fermi level would be shifted well beyond the local minimum in the DOS [see Fig. 4(a)], resulting in an increase in N_s and thus in a positive ΔT_c, which is not the experimental result. The increase of d_s and the consequent existence of an upper limit for Δn_{3D} are thus qualitatively independent on the details of the proximity effect model [28]. For larger values of Δn_{2D}, d_s further expands, finally reaching 4–5 unit cells. For $\Delta n_{2D} > 5 \times 10^{14}$ cm^{-2} the dependence of d_s on Δn_{2D} is remarkably linear. Note that the increase in d_s is not fast enough to keep the volume density of induced electrons Δn_{3D} constant [see Fig. 4(c)]; in this range, Δn_{3D} increases from 1×10^{22} cm^{-3} ($\sim$0.2 e^-/u.c.) and tends to saturate around 2×10^{22} cm^{-3} ($\sim$0.4 e^-/u.c.).

These results suggest that Δn_{3D} cannot exceed 2×10^{22} cm^{-3} ($\sim$0.4 e^-/u.c.), and that the thickness of the surface layer departs from a Thomas-Fermi value [see Fig. 4(b)] when Δn_{3D} approaches this limit [see Fig. 4(c)], as if the surface layer of thickness $\approx \lambda_{TF}$ was unable to accommodate all the induced charges. To look for an explanation of this effect, one has to abandon the Thomas-Fermi approximation: In this high charge-density regime the assumptions of weak perturbation and linear response are no longer valid since the surface potential $\phi(z = 0)$ does no longer fulfill the condition $|e\phi(z = 0)| \ll E_F$. The screening theory beyond the linear regime [40] correctly explains the observed increase of d_s up to about 3.6 Å when $\Delta n_{2D} \simeq 5 \times 10^{14}$ cm^{-2}, but above this doping value the appropriate theory is lacking [28].

In summary, we have experimentally proven that a *surface* charge induced by electrochemical gating can give rise to modifications of the *bulk* superconducting properties (and not only of the surface ones). This is true, surprisingly, in conventional BCS-like superconductors with a large electronic screening, and can be explained in terms of a proximity effect between the surface layer and the underlying part of the sample. We have also unveiled an increase in the effective electronic screening length that departs from the Thomas-Fermi value and increases, suggesting the existence of an upper limit for the volume charge density. These findings severely impact the study of the effects of EDL gating on high-carrier-density systems in general, and metallic superconductors in particular.

[1] S. Jo, D. Costanzo, H. Berger, and A. F. Morpurgo, Nano Lett. **15**, 1197 (2015).

[2] K. Ueno, S. Nakamura, H. Shimotani, A. Ohtomo, N. Kimura, T. Nojima, H. Aoki, Y. Iwasa, and M. Kawasaki, Nat. Mater. **7**, 855 (2008).

[3] J. T. Ye, Y. J. Zhang, R. Akashi, M. S. Bahramy, R. Arita, and Y. Iwasa, Science **338**, 1193 (2012).

[4] J. T. Ye, S. Inoue, K. Kobayashi, Y. Kasahara, H. T. Yuan, H. Shimotani, and Y. Iwasa, Nat. Mater. **9**, 125 (2010).

[5] K. Ueno, S. Nakamura, H. Shimotani, H. T. Yuan, N. Kimura, T. Nojima, H. Aoki, Y. Iwasa, and M. Kawasaki, Nat. Nanotechnol. **6**, 408 (2011).

[6] D. Daghero, F. Paolucci, A. Sola, M. Tortello, G. A. Ummarino, M. Agosto, R. S. Gonnelli, J. R. Nair, and C. Gerbaldi, Phys. Rev. Lett. **108**, 066807 (2012).

[7] H. Nakayama, J. T. Ye, T. Ohtani, Y. Fujikawa, K. Ando, Y. Iwasa, and E. Saitoh, Appl. Phys. Exp. **5**, 023002 (2012).

[8] M. Tortello, A. Sola, K. Sharda, F. Paolucci, J. R. Nair, C. Gerbaldi, D. Daghero, and R. S. Gonnelli, Appl. Surf. Sci. **269**, 17 (2013).

[9] J. Shiogai, Y. Ito, T. Mitsuhashi, T. Nojima, and A. Tsukazaki, Nat. Phys. **12**, 42 (2016).

[10] B. Lei, J. H. Cui, Z. J. Xiang, C. Shang, N. Z. Wang, G. J. Ye, X. G. Luo, T. Wu, Z. Sun, and X. H. Chen, Phys. Rev. Lett. **116**, 077002 (2016).

[11] X. X. Xi, H. Berger, L. Forró, J. Shan, and K. F. Mak, Phys. Rev. Lett. **117**, 106801 (2016).

[12] M. Yoshida, J. T. Ye, T. Nishizaki, N. Kobayashi, and Y. Iwasa, Appl. Phys. Lett. **108**, 202602 (2016).

[13] L. J. Li, E. C. T. O'Farrell, K. P. Loh, G. Eda, B. Özyilmaz, and A. H. Castro Neto, Nature (London) **529**, 185 (2016).

[14] A. T. Bollinger, G. Dubuis, J. Yoon, D. Pavuna, J. Misewich, and I. Božović, Nature (London) **472**, 458 (2011).

[15] X. Leng, J. Garcia-Barriocanal, S. Bose, Y. Lee, and A. M. Goldman, Phys. Rev. Lett. **107**, 027001 (2011).

[16] X. Leng, J. Garcia-Barriocanal, B. Yang, Y. Lee, J. Kinney, and A. M. Goldman, Phys. Rev. Lett. **108**, 067004 (2012).

[17] S. Maruyama, J. Shin, X. Zhang, R. Suchoski, S. Yasui, K. Jin, R. L. Greene, and I. Takeuchi, Appl. Phys. Lett. **107**, 142602 (2015).

[18] K. Jin, W. Hu, B. Zhu, D. Kim, J. Yuan, Y. Sun, T. Xiang, M. S. Fuhrer, I. Takeuchi, and R. L. Greene, Sci. Rep. **6**, 26642 (2016).

[19] J. Walter, H. Wang, B. Luo, C. D. Frisbie, and C. Leighton, ACS Nano **10**, 7799 (2016).

[20] A. Fête, L. Rossi, A. Augieri, and C. Senatore, Appl. Phys. Lett. **109**, 192601 (2016).

[21] J. Jeong, N. B. Aetukuri, T. Graf, T. D. Schladt, M. G. Samant, and S. S. P. Parkin, Science **339**, 1402 (2013).

[22] M. Li, W. Han, X. Jiang, J. Jeong, M. G. Samant, and S. S. P. Parkin, Nano Lett. **13**, 4675 (2013).

[23] T. D. Schladt, T. Graf, N. B. Aetukuri, M. Li, A. Fantini, X. Jiang, M. G. Samant, and S. S. P. Parkin, ACS Nano **7**, 8074 (2013).

[24] R. E. Glover and M. D. Sherrill, Phys. Rev. Lett. **5**, 248 (1960).

[25] H. L. Stadler, Phys. Rev. Lett. **14**, 979 (1965).

[26] J. Choi, R. Pradheesh, H. Kim, H. Im, Y. Chong, and D. H. Chae, Appl. Phys. Lett. **105**, 012601 (2014).

[27] A. Nigro, G. Nobile, M. G. Rubino, and R. Vaglio, Phys. Rev. B **37**, 3970 (1988).

[28] See Supplemental Material at http://link.aps.org/supplemental/10.1103/PhysRevB.95.140501 for further details on device fabrication and characterization, the measurement technique, DFT calculations, and the theoretical models for the proximity effect and the electrostatic screening beyond the linear regime.

[29] Z. Wang, A. Kawakami, Y. Uzawa, and B. Komiyama, J. Appl. Phys. **79**, 7837 (1996).

[30] A. Semenov, B. Günther, U. Böttger, H. W. Hübers, H. Bartolf, A. Engel, A. Schilling, K. Ilin, M. Siegel, R. Schneider, D. Gerthsen, and N. A. Gippius, Phys. Rev. B **80**, 054510 (2009).

[31] P. Gallagher, M. Lee, T. A. Petach, S. W. Stanwyck, J. R. Williams, K. Watanabe, T. Taniguchi, and D. Goldhaber-Gordon, Nat. Commun. **6**, 6437 (2015).

[32] G. Inzelt, in *Electroanalytical Methods. Guide to Experiments and Applications*, edited by F. Scholz (Springer, Berlin, 2010), pp. 147–158.

[33] E. Piatti, A. Sola, D. Daghero, G. A. Ummarino, F. Laviano, J. R. Nair, C. Gerbaldi, R. Cristiano, A. Casaburi, and R. S. Gonnelli, J. Supercond. Novel Magn. **29**, 587 (2016).

[34] T. Koyama, Phys. Rev. B **70**, 226503 (2004).

[35] J. E. Hirsch, Phys. Rev. B **70**, 226504 (2004).

[36] P. G. de Gennes, Rev. Mod. Phys. **36**, 225 (1964).

[37] L. N. Cooper, Phys. Rev. Lett. **6**, 689 (1961).

[38] W. Silvert, Phys. Rev. B **12**, 4870 (1975).

[39] S. P. Chockalingam, M. Chand, J. Jesudasan, V. Tripathi, and P. Raychaudhuri, Phys. Rev. B **77**, 214503 (2008).

[40] J.-N. Chazalviel, *Coulomb Screening by Mobile Charges: Applications to Materials Science, Chemistry, and Biology* (Springer, New York, 1999).